



Infrared Spectroscopic Measurements of the Structure of Organic Thin Films; Furfural on Pd(111) and Au(111) Surfaces

Journal:	<i>CrystEngComm</i>
Manuscript ID	CE-ART-04-2021-000565.R1
Article Type:	Paper
Date Submitted by the Author:	03-Jun-2021
Complete List of Authors:	Bavisotto, Robert; University of Wisconsin-Milwaukee College of Letters and Science, Chemistry and Biochemistry Hopper, Nicholas; University of Wisconsin-Milwaukee, Chemistry and Biochemistry Boscoboinik, Alejandro; University of Wisconsin-Milwaukee, Chemistry and Biochemistry Owen, Quintus; University of Wisconsin-Milwaukee, Chemistry and Biochemistry Tysoe, W.; University of Wisconsin-Madison, Chemistry and Biochemistry

Infrared Spectroscopic Measurements of the Structure of Organic Thin Films; Furfural on Pd(111) and Au(111) Surfaces

by

Robert Bavisotto, Nicholas Hopper, Alejandro Boscoboinik, Quintus Owen and Wilfred T. Tysoe*

Department of Chemistry and Biochemistry, University of Wisconsin-Milwaukee, Milwaukee, WI 53211, USA

Abstract

Electron and X-ray diffraction (XRD) and electron microscopy are predominantly used to investigate the structures of thin organic films deposited from the vapor at low temperatures on planar substrate to obtain the crystal structure of the thin film. This work illustrates how the structure of films on a metal substrates can be continually monitored both during growth and as it is annealed until the film desorbs using reflection-absorption infrared spectroscopy (RAIRS). The chemical nature of the film, including molecular conformations, can be determined from the vibrational frequencies of the organic film, and the film orientation can be obtained using the infrared selection rules for reflective surfaces, which states that only those vibrational modes with a vibrational component perpendicular to the surface are detected. The approach is illustrated for furfural adsorbed on an unreactive metal, gold, and a more reactive one, palladium, to gauge the effect of substrate reactivity on the film structure. Furfural is chosen as a test molecule because it is planar, has two conformations depending on the orientation of the aldehyde group relative to the furyl ring, and the film structure has been studied by XRD. It is found that only the structure of the first layer in contact with the surface is influenced by the nature of the substrate. Changes in the ratio of the cis and trans conformation as well as changes in the degree of order of the furfural film are found as a function of film thickness and temperature.

Keywords: furfural, Au(111). Pd(111), reflection absorption infrared spectroscopy, thin-film structure

* Author to whom correspondence should be addressed

Introduction

Organic thin films are extensively used for applications such as thin-film transistors¹⁻³ or for organic light-emitting devices,⁴ and therefore understanding the structures of organic thin films is essential to designing such devices. The crystalline structure of these thin films can be measured using electron⁵ or X-ray diffraction by cryocrystallography⁶ or, more recently, by electron microscopy.⁷ An alternative, nondestructive approach is to use reflection-absorption infrared spectroscopy (RAIRS) to investigate the structure and properties of thin organic films during in-situ growth and while heating to rapidly map the structural transformations to identify conditions for making more detailed diffraction measurements. In particular, the selection rules for infrared absorption on a metal substrate^{8, 9} help determine molecular orientations, while the vibrational frequency shifts are also sensitive to the molecular conformation.¹⁰ This approach is illustrated here using thin molecular films of furfural (FF, C₅H₄O₂) adsorbed on metal substrates at low temperature (~90 K), and by heating them slowly to observe the structural changes that occur while heating. Furfural is essentially planar, although the aldehyde group can rotate relative to the furyl ring so that furfural can exist in two conformers depending on whether the aldehyde carbonyl group is adjacent to (cis) or distal from (trans) the furan ring oxygen as portrayed in Figure 1. The assigned gas-phase infrared spectrum of furfural demonstrates that these two conformations can be easily distinguished spectroscopically from their vibrational frequency shifts.^{11, 12} It has been found that furfural exists primarily as the trans conformation in the vapor phase,¹³ but largely in the cis conformation in the liquid phase, and exclusively as cis in the solid.¹² In the following, the coverage- and temperature-dependent spectra are collected continuously as the substrates are dosed from the background or slowly heated. This allows the film structure to be continually monitored and also minimizes the total experimental time thereby minimizing the background shift

due to slow changes in the background spectrum. The detailed information obtained in this way can also be used to obtain kinetic parameters such as the activation energies for structural transformations on the surface.

RAIRS results are supplemented by temperature-programed desorption (TPD) experiments to establish the temperature at which multilayer desorb from the surface to aid in infrared assignments. The film structures of furfural on a reactive Pd(111) surface are compared with adsorption on a more chemically inert Au(111) substrate to investigate how surface interactions might influence the structure of the organic films deposited on them. The RAIRS experiments also show crystallization of the film at low temperatures when sufficiently thick multilayers are present, and the surface selection rules provide information on the structure and orientation of the resulting film. Finally, the results are compared to the X-ray diffraction (XRD) structural measurements for crystalline thin films of furfural reported previously ⁶ that show furfural crystals formed at ~232 K contain only the cis isomer. This crystal structure was measured above the temperature at which furfural multilayers desorb in ultrahigh vacuum so presumably exists in equilibrium with the vapor in the XRD experiments.

It should be mentioned that furfural has been used as a model feedstock for biomass conversion. To produce value-added products from lignocellulosic biomass, the raw materials (cellulose, hemicellulose) are typically hydrolyzed to the corresponding carbohydrate monomers (glucose, fructose, and xylose) using acid catalysis.¹⁴⁻¹⁷ Subsequent acidic dehydration leads to the formation of smaller oxygenates such as furfural, 5-hydroxymethylfurfural (HMF), and levulinic acid (LA). These products can be used to produce fuels and polymers or for synthesizing other monomers relevant to the polymer industry.^{15, 17-22}

Experimental Methods

Experiments were carried out in ultrahigh vacuum (UHV) chambers operating at base pressures of $\sim 2.0 \times 10^{-10}$ Torr after bakeout. Infrared spectra were collected using a Bruker Vertex 70 infrared spectrometer using a liquid-nitrogen-cooled, mercury cadmium telluride detector.²³ The complete light path was enclosed and purged with dry, CO₂-free air. Spectra were collected for 1000 scans at 4 cm⁻¹ resolution and the surface was exposed to furfural using a precision variable leak valve connected to the infrared cell. Rather than measuring the infrared spectra sequentially after dosing the sample, spectra were collected while exposing the sample to furfural, where the dosing pressure was set to be sufficiently low that the coverage only varied slightly during the time it took to collect a spectrum. Temperature-ramp experiments were performed by precisely controlling the sample temperature by regulating the heating current from a Kepco model ATE 6-50M DC power supply using a homemade Labview program, which was controlled by a National Instruments card, model USB-6001. This allowed stable and accurately controllable temperature ramps to be obtained and the infrared spectra were collected continually as the temperature was varied. The sample temperature was monitored by means of a chromel/alumel thermocouple spot-welded to the edge of the single crystal, enabling the temperature to be accurately controlled and ramped at a precise rate of 0.5 K/minute. Since it requires ~ 4 minutes to collect an infrared spectrum, the temperature varied only by ~ 2 K while collecting each spectrum. This experimental strategy also minimized the total experimental time and so limited the drift in the clean-surface background spectrum. Integrated absorbances of selected infrared peaks were measured by first subtracting a small, smoothly varying background from the spectra, which was generally much lower than the peaks absorbances for the furfural multilayers, even for temperature-dependent spectra (see Fig. S3).

TPD data were collected at a heating rate of $\sim 5\text{K}/\text{second}$ with products being detected using a Hiden HAL 301 quadrupole mass spectrometer placed close to the front of the Pd(111) single crystal, which was dosed with furfural at $\sim 140\text{ K}$.

The Pd(111) sample was cleaned using a standard procedure of Ar^+ bombardment with subsequent heating in oxygen to remove any strongly bound surface carbon. Ar^+ bombardment was performed at a background pressure $\sim 3.0 \times 10^{-5}$ Torr at a 1 kV potential, while maintaining a $\sim 2\ \mu\text{A}$ sample current. Cycles of heating were performed in a background pressure of $\sim 3.0 \times 10^{-8}$ Torr of oxygen at a sample temperature of 780 K for 10 minutes. The sample was cooled to 690 K and flash annealed to 850 K to desorb any remaining adsorbates. After completing three cycles of heating in oxygen, cooling, then annealing, the sample was allowed to cool to $\sim 400\text{ K}$, after which the oxygen exposure was stopped and the sample was flash annealed to 1000 K while subsequently scanning using a Hiden mass spectrometer and monitoring the CO (28 amu) versus O_2 (32 amu) signal ratio. When the oxygen signal intensity significantly exceeded the CO signal, the Pd(111) sample was considered to be free of carbon, particularly in the subsurface region of the sample. This process was repeated three times before conducting each experiment.

The Au(111) sample was cleaned using a standard procedure of Ar^+ bombardment for 30 minutes. This was followed by briefly heating to 900 K for 5 minutes and subsequently annealing to 700 K for 30 minutes. This cleaning procedure was repeated until the sample was found to be clean by Auger electron spectroscopy.

Furfural (Aldrich, $> 99.9\%$ purity) was purified using several freeze-pump-thaw cycles, its cleanliness judged by mass spectroscopy, and then dosed using a variable leak valve via a 3.2-mm internal diameter tube with the end located relatively close to the front of the sample, but far enough away to produce a relatively uniform flux across the sample. This arrangement limits the

contamination of other parts of the UHV chamber and enhances the local pressure at the sample. An enhancement factor of 100 was applied to calculate all exposures. Exposures in Langmuirs ($1 \text{ L} = 1 \times 10^{-6} \text{ Torr}\cdot\text{second}$) were not corrected for ionization gauge sensitivities.

The furfural vibrational frequencies were calculated using periodic density functional theory (DFT) using the projector augmented wave (PAW) method as implemented in the Vienna ab-initio simulation package (VASP) code.^{24, 25} The exchange and correlation energies were calculated using the PBE3 (Perdew, Burke and Ernzerhof) form of the generalized gradient approximation (GGA).²⁶ The kinetic energy cutoff for all calculations was 400 eV. The wavefunctions and electron density were converged to within 1×10^{-5} eV, while geometric structures were optimized until the forces on the atoms were less than 0.01 eV/Å. Van der Waals' interactions were implemented using the DFT-D3 method as described by Grimme et al.²⁷ The Brillouin zone was sampled using a Γ -centered Monkhorst-Pack ($1 \times 1 \times 1$) k-point mesh.²⁸ The molecule was first allowed to relax in a sufficiently large cell ($36 \times 36 \times 36$) and the vibrational frequencies were tabulated and mass displacement vectors were added and analyzed using imaging software Vesta (Figs. S1 and S2).²⁹

Results

Infrared Spectroscopy of Furfural Adsorption

The surface and thin-film chemistry of furfural was investigated on surfaces of both Pd(111) at 90 K and Au(111) at 130 K by adsorbing furfural onto the cooled single crystal and continually collecting the infrared spectra while dosing to provide a complete picture of the structural evolution of the film as a function of exposure. The infrared spectra for furfural uptake are shown in Figure 2 for Au(111) and in Figure 4 for Pd(111).

Infrared features are assigned by comparison both with previous studies of the infrared spectra of molecular furfural^{11, 12, 30} as well as the results of DFT calculations, and the vibrational assignments are summarized in Table 1. The resulting normal modes are depicted in the Supplemental Information section (Figs. S1 and S2), and the symmetry assignments of the normal modes within the C_s point group are included in Table 1. Frequencies of the multilayer spectra, obtained following a 140.9 L exposure on Au(111) (Fig. 2) and a 46.8 L exposure on Pd(111) (Fig. 4), are in good agreement with those of gas-phase furfural, which confirms molecular adsorption onto both surfaces below 130 K. The majority of the normal modes of furfural have A' symmetry, which transform as vectors lying within the plane of the furfural molecule, while only two observed modes have A'' symmetry, which transforms as a vector that is perpendicular to the furfural molecular plane, due to out-of-plane vibrations at 842 and 799 cm^{-1} .

Coverage-Dependent Structural Transformations

The molecular conformation can also be distinguished from shifts in the frequencies of some vibrational modes depending on whether the aldehyde carbonyl group is cis (Fig. S1) or trans (Fig. S2) to the furyl ring oxygen (Fig. 1). This effect is most prominent in the carbonyl stretching modes, where the 1703 cm^{-1} mode is due to the cis conformer, while the 1677 cm^{-1} peak is assigned to the trans structure. Other features that show similar cis-trans splitting are the 1475/1465 cm^{-1} doublets due to a furyl ring breathing mode, as well as the 1279/1251, 1230/1207 and 929/947 cm^{-1} doublets due to C–H in-plane bending vibrations, where the first vibrational frequency is due to the cis conformer and the latter to the trans geometry.

At low coverages on Au(111) (Fig. 2) and Pd(111) (Fig. 4), the spectra exhibit only furfural A'' modes at 799 cm^{-1} without any accompanying A' modes, indicating that furfural adopts a flat-

lying geometry. The absence of signals due to vibrations with A' symmetry persists until exposures of ~ 1.3 L for gold and ~ 1.6 L for palladium. At higher exposures, the furfural carbonyl modes at $1703/1677\text{ cm}^{-1}$, and the A' and A'' symmetry modes grow in intensity, indicating that adsorbed furfural starts to tilt. These structural transformations are analyzed in greater detail for furfural adsorbed on a more inert Au(111) surface as shown in Figure 3, obtained by fitting selected peaks to obtain values of their integrated absorbances.

Figure 3A shows the intensity variation of modes with A' symmetry from the intense furyl ring vibration at 1470 cm^{-1} (■) compared to a mode of A'' symmetry at 781 cm^{-1} (●). The behavior can be split into three regions, I, II and III, as indicated on Fig. 3A. Region I occurs between 0 and ~ 1.3 L exposure, where the furfural out-of-plane A'' modes at 781 cm^{-1} increase in intensity without any corresponding increase in the absorbance of the A' mode at 1470 cm^{-1} indicating the presence of flat-lying furfural. Region II occurs as the exposure exceeds ~ 1.3 L, where the A' modes subtly increase in intensity signifying the onset of formation of a tilted structure on the crowded surface. The relative proportions of cis and trans furfural conformers were measured from the integrated absorbances of the $1475/1465\text{ cm}^{-1}$ doublet and the results are displayed in Fig. 3B. At an exposure of 1 L (region I), furfural comprises $\sim 67\%$ trans (●) and 33% cis (■) conformer. As the furfural coverage increases (region II), the proportion of trans furfural increases. As will be shown below, the trans-to-cis interconversion begins at ~ 180 K, 50 K higher than the sample temperature used to collect the data shown in Figure 3. This implies that the cis-to-trans ratio of furfural adsorbed at temperatures well below the transition temperature reflects the cis-to-trans ratio of the vapor. If this is the case, the apparent change in cis-to-trans ratio during furfural adsorption is not interconversion of the isomers, but the change in infrared intensity is a result of orientation changes of adsorbed furfural, with the cis conformer being more perpendicular to the

surface. DFT calculations indicate that flat-lying and bent-trans furfural are more strongly adsorbed on Pd(111) than the cis conformer by ~ 0.1 - 0.2 eV.^{31, 32} The absorbance changes due to changes in average tilt angle as a result of the IR surface selection rules^{8, 9} would account for a higher apparent proportion of cis conformer, rather than reflecting a true change in the conformer ratio. As shown in figure 3B, the ratio tends asymptotically to 75% trans, 25% cis in the multilayer and is constant after the onset of region III.

Shown in Fig. 3C are the carbonyl peak frequencies for the cis (~ 1700 cm^{-1} , ■) and trans (~ 1677 cm^{-1} , ●) conformers as a function of furfural exposure. At the lowest coverages (region I), the carbonyl species lie close to parallel to the surface, but the absorption cross section is sufficiently large that the peak can still be detected. The trans carbonyl mode appears at ~ 1701 cm^{-1} at the lowest coverage, but shifts to 1700 cm^{-1} as the exposure increases to ~ 3 L, while the carbonyl vibrational frequency of the cis conformer shifts from ~ 1668 cm^{-1} at low coverages to 1673 cm^{-1} as the exposure exceeds 3 L. This shift at lower coverages is attributed to the different interactions of flat-lying and tilted furfural with the surface. The onset of the formation of furfural multilayers is difficult to identify unequivocally from the IR data, but comparing the intensity of the carbonyl modes of the remaining monolayer post multilayer desorption after briefly heating to 179 K (Fig. 8) with the adsorption spectra of ~ 2.9 L at 90K (Fig. 4), suggests that the monolayer growth is complete at this exposure and the multilayer then starts to form.

The average furfural tilt angle with respect to the surface was estimated from the relative intensities of the A' (1470 cm^{-1}) and the A'' modes (781 cm^{-1}) by using calculated absorbance values in the literature.¹³ Figure 3D shows the resulting average furfural tilt angle for exposures above ~ 1.3 L (region II). Furfural adopts a flat-lying geometry for a less than 1.3 L exposure (region I), but tilts as the exposure exceeds this value (region II). The tilt angle increases rapidly

as the surface becomes more crowded to reach an angle of $\sim 35^\circ$ at an exposure of ~ 3 L and continues to increase towards a value of $\sim 54^\circ$, close to the magic angle, at higher exposures and implies that the furfural is randomly oriented in the multilayer. The deviation from 54° for exposures between 3 L for the saturated monolayer and 10 L exposure (region III) reflects the transition from a flat-lying species, to tilted furfural at $\sim 40^\circ$ ^{31,32} at intermediate coverages, to the randomly oriented multilayer at 54° .

Figure 4 shows the corresponding infrared spectra for furfural adsorbed on Pd(111) at 90 K. The low-temperature behavior is very similar to that found on Au(111) at 130 K, described above. The furfural A'' modes dominate at the lowest coverages, followed by the appearance of A' modes at higher exposures. More subtle changes become apparent when the results are plotted as shown in Figure 5, which exhibit similar variations with exposure as seen in Fig. 3, indicating that the reactivity of the different substrates does not significantly influence the low-temperature structures of furfural. Figure 5A plots the integrated intensities of the 1470 (A' symmetry, ■) and 781 cm^{-1} (A'' symmetry, ●) features versus exposure, again demonstrating that adsorption occurs on Pd(111) in three distinct regions. Region I occurs between 0 and 1.6 L where furfural adopts a flat-lying orientation and only modes of A'' symmetry are detected. Region II occurs for exposures >1.6 L where the A' vibrations at 1470 cm^{-1} intensify. Region III starts at an exposure of ~ 10 L and is evident from the constant cis/trans ratio shown in Fig. 5C and from the constant growth rate of the A' and A'' modes shown in Fig. 5B. At the lowest coverages on Pd(111), furfural comprises 65% trans conformer and, as the exposure increases to 10 L and above, the distribution stabilizes at $\sim 75\%$ trans-FF, 25% cis-FF. This is ascribed to the slightly greater stability of the flat-lying trans conformer^{31,32} as discussed above. Figure 5D shows the average furfural tilt angle as a function of exposure. At the lowest coverages, the absence of A' modes (Fig. 4) indicate the presence of

only flat-lying furfural. As the exposure increases to 3 L, the furfural angle increases to $\sim 35^\circ$ due to the presence of a tilted structure on the crowded surface. At higher exposures, the formation of a furfural multilayer is inferred from the average tilt angle of $\sim 54^\circ$ as discussed above.

The above assignment allows thickness of each furfural film to be estimated by comparing the intensities of carbonyl modes of the furfural monolayer to the intensities during adsorption and indicate that the final thicknesses of the furfural films are ~ 47 monolayers (ML) on Au(111) (Fig. 2) and ~ 16.7 ML on Pd(111) (Fig. 4).

Temperature-Dependent Evolution of Furfural Structures

The effect of heating furfural multilayers was investigated by continually collecting RAIRS spectra while slowly ramping the temperature. The RAIR spectra of furfural multilayers adsorbed on Au(111) at 130 K (Figure 6, ~ 47 ML) and on Pd(111) at 90 K (Figures 8, ~ 16.7 ML and 10, ~ 9.1 ML) were collected as a function of temperature from the adsorption temperature to the multilayer furfural desorption temperature (~ 175 K).

The spectra generally evolve similarly on both substrates, indicating that the behavior is not strongly influenced by the nature of the substrate. Several structural transformations occur and are documented in Figures 7, 9, and 11, which plot the temperature dependences of various parameters and can be divided into five distinct temperature regions for each film. The first region (region I) occurs between the adsorption temperature and ~ 140 K where there are no significant changes in intensity or vibrational frequency. This observation justifies the postulate made above that there is no change in cis-to-trans ratio during furfural adsorption at sufficiently low temperatures. The spectra collected over this temperature range are omitted from Figs. 6, 8 and 10 for clarity. Between 140 and 160 K (region II, Figs. 6 and 8), the A'' mode (784 cm^{-1}) intensity decreases,

while the carbonyl modes near 1700 cm^{-1} intensify. Between 150 and 160 K (region III), the cis-to-trans ratio starts to favor the cis species, while heating to 165 K (region IV) causes the A' vibrations and carbonyl stretching modes to decrease drastically in intensity, while the A'' modes intensify. This trend continues until the onset of desorption (region V) at $\sim 170\text{ K}$, when all infrared features disappear. These changes are detailed in Figs. 7 and 9 and are described in greater detail below.

Temperature Dependence of Furfural Multilayers on Gold

The furyl ring breathing modes at $\sim 1470\text{ cm}^{-1}$ were analyzed in the most detail to illustrate how the FF cis/trans ratio changes with temperature on the Au(111) surface. The integrated absorbances of the individual components were measured by fitting to two Gaussian profiles and the results are plotted in Fig. 7A. Figure 7B shows the resulting temperature dependence of the proportion of cis (■) and trans (●) species. This reveals that, between 140 and 160 K (regions II and III), furfural converts from the trans to cis conformer, and subsequently starts to lay flat at 160 K.

Figure 7C plots the average furfural tilt angle as a function of temperature showing that heating to 145 K causes the furfural tilt angle to increase to $\sim 75^\circ$ with respect to the surface. Since the conversion from the trans to the cis conformer starts at this temperature, it may be facilitated by an orientation change. Heating to 155 K causes a significant decrease in the furfural tilt angle to form an almost flat-lying species, with an average tilt angle of $\sim 18^\circ$. The temperature intervals are sufficiently small that they enable the temperature variation of the cis-to-trans FF ratio to be measured as a function of sample temperature and Fig. 7D shows the resulting Arrhenius plot obtained from the features at 1470 cm^{-1} (Fig. 7A) to yield a slope of -4.3 ± 0.3 .

Temperature Dependence of Furfural Multilayers on Palladium

The temperature dependences of furfural on Pd(111) are shown in Fig. 8 where the furfural ring breathing modes at $\sim 1470\text{ cm}^{-1}$ were used to gauge the cis/trans composition for the 16.7-ML thick film on Pd(111) (Fig. 9A). The results are converted to percentage of cis and trans conformers in Fig. 9B. The behavior is similar to that found for furfural on Au(111) (Fig. 7B) where the conversion to the cis conformation starts at $\sim 145\text{ K}$, prior to then converting to flat-lying species.

Figure 9C plots the cis/trans ratio over a larger temperature range. The ratio is constant from 90 to 140 K, but then increases rapidly at $\sim 140\text{ K}$ to form mostly the cis conformer. Above 160 K, the cis and trans components of the 1470 cm^{-1} features become more difficult to identify, but the composition quickly shifts towards containing predominantly the trans conformer as the multilayer desorbs. One possible explanation for this is that the monolayer in contact with the palladium surface does not participate in the cis/trans conversion and the overlayer that contains only cis species desorbs, resulting in the observed proportion of the trans conformer increasing. Fig. 9D shows the corresponding temperature dependence of the tilt angle of a $\sim 16.7\text{ ML}$ furfural film on Pd(111). Similar to the behavior on Au(111), the furfural multilayer has a tilt angle of $\sim 54^\circ$ due to the presence of a randomly adsorbed film, but heating causes an increase in angle to $\sim 70^\circ$ at a temperature coincident with trans-to-cis conversion (Fig. 9C). Heating to 155 K causes the tilt angle to decrease to $\sim 10^\circ$ to form a flat-lying species, which desorbs at $\sim 170\text{ K}$. The remaining infrared signals, which are difficult to see in Fig. 8 due to the scale, are due to the chemisorbed monolayer. This behavior is different from furfural on Au(111) where the monolayer desorbs coincident with the multilayer. The different responses of the surfaces are mainly restricted to the

monolayer because the structure and properties of the multilayer film are independent of the substrate.

The effect of furfural multilayer thickness was investigated for a thinner furfural film by depositing ~ 9.1 ML of furfural on Pd(111), where the temperature-dependent spectra are shown in Figure 10. For this thinner film, the decrease in intensity of the A' mode is not accompanied by an increase in A'' mode intensity, but rather results from furfural desorption (region V). Another interesting point is that the shoulders on the carbonyl modes, centered at 1666 cm^{-1} , are absent when heating this film. It can be assumed that this peak, present in Figs. 6 and 8, is an overtone of the strong peak at 783 cm^{-1} so that the shift to 1666 cm^{-1} from the theoretical value 1566 cm^{-1} is likely due to a Fermi resonance. The detailed temperature-dependent plots shown in Figure 11 reveal that this thinner film behaves similarly to the thicker 16.7 ML film, but with some exceptions. Figure 11A plots the furfural cis and trans distribution as a function of temperature and shows that the interconversion occurs over the same temperature range as the thicker film. In addition, the furfural tilt angle changes over the same temperature range as the thicker film (compare Figs. 11B and 9D). As the temperature exceeds 130 K, the furfural tilt angle increases to $\sim 70^\circ$, coincident with a change in conformation so that the main difference between the 9.1 and 16.7 ML films is that the furfural does not undergo a significant decrease in tilt angle for the thin film, but is tilted at 70° until it desorbs and decreases to $\sim 50^\circ$, close to the value found for the monolayer. Figure 11C shows an Arrhenius plot of the cis/trans ratio for the 9.1 ML film, where the slope is -3.79 ± 0.23 .

Finally, TPD data were collected for furfural multilayers on Pd(111) at a heating rate of 5 K/s (Fig. 12), while monitoring the 96 amu signal, the parent mass of furfural, as a function of

exposure. No decomposition products were observed over this temperature range. The furfural films desorb in two peaks centered at ~ 173 K and a broader peak centered at ~ 195 K.

Discussion

Infrared Spectroscopy of Furfural Adsorption

At low furfural coverages on Pd(111), the intensity of peaks of A'' symmetry vibrations increases without any accompanying increase in the A'-mode intensity, indicating that the furfural adsorbs in a flat-lying configuration due to the interaction of the skeletal π -orbitals with the substrate. The associated aldehyde C-H rocking mode at ~ 1367 cm^{-1} is still evident for the flat-lying species, confirming that the furfural is intact and that this mode has a component of its vibration perpendicular to the surface. In addition, peaks at 1571 and 1465 cm^{-1} suggest that the furyl ring is not perfectly parallel to the Pd(111) surface in this close-to flat-lying species. The vibrational frequencies of the sub-multilayer structures are in accord with the group frequencies expected for 2-substituted furans, which are characterized by peaks at 1605 to 1570 cm^{-1} (1571 cm^{-1} in furfural), 1510 to 1475 cm^{-1} (1465 cm^{-1} in furfural) and from 1400 to 1380 cm^{-1} (1395 cm^{-1} in furfural).¹⁰ In particular, the carbonyl stretching modes of the tilted monolayer species are close to those found in the large multilayer (Figure 2), implying that the aldehyde group is not significantly shifted by interaction with the palladium or gold surfaces,^{33, 34} indicating that the carbonyl groups are remote from the surface in the tilted structures. DFT calculations identify two types of tilted species on Pd(111):^{31, 32} a so-called Tilted-1 species, in which the furfural adsorbs via the CHO group binding to the Pd(111) surface, and a Tilted-2 species, which adsorbs via the furan ring. Both are predicted to have a molecular tilt angle of $\sim 35^\circ$ to the surface but since the

spectra of furfural on Pd(111) show no significant shifts in the carbonyl stretching modes or the A'' CHO mode, this suggests that it adsorbs in the Tilted-2 configuration and binds via the ring.

For exposures greater than ~ 1.3 L on Au(111) and greater than ~ 1.6 L on Pd(111), modes with A' symmetry begin to grow as shown in Figures 3 and 5. Fitting and integrating the cis/trans doublet at ~ 1470 cm^{-1} allow the cis and trans distribution to be estimated and reveals that, during adsorption, the furfural is $\sim 70\%$ trans and $\sim 30\%$ cis. The detection of both A' and A'' modes in the multilayer indicates that furfural is not lying flat at higher exposures. Compared to the spectrum of liquid furfural,³⁵ the thin-film spectra have different relative intensities of modes with A'' symmetry at 784 cm^{-1} and the carbonyl modes at 1700 cm^{-1} , where the A'' modes are more intense relative to the carbonyl stretching modes in the thin films compared to the liquid. This indicates that the furfural in the thin films has a greater tendency to be oriented parallel to the substrate than in an isotropic liquid.

The average tilt angle was calculated from the variation in intensity of A' (at 1465 cm^{-1}) and A'' (784 cm^{-1}) modes as a function of coverage, by calibrating the intensities using the absorbance values in literature.¹³ The results are displayed in Figures 3D and 5D for ~ 47 ML films on Au(111) and 16.7 ML films on Pd(111). Note that the tilt angle varies with exposure, tending to an asymptotic value of $\sim 54^\circ$, where the A'' modes appear at lower coverages than the A' modes, as discussed above, due to furfural being almost parallel to the surface at low coverages. Surface crowding at higher coverage causes the furfural to tilt to $\sim 40^\circ$,³⁶ then to convert to a randomly oriented multilayer for exposures above 3 L, with an average tilt angle of $\sim 54^\circ$ for random adsorption. The variation from flat-lying to tilted species is common for planar π -conjugated molecules adsorbed on metal surfaces and was first discovered for benzene on Pd(111)^{36,37} where the change in orientation, while it decreases the heat of adsorption for individual molecules, cause

an overall reduction in surface energy. Multilayer adsorption of furfural on Pd(111) commences after a $\sim 3L$ furfural exposure at a sample temperature of 90 K, and at $\sim 3L$ on the Au(111) sample at 130 K.

Temperature-Dependent Evolution of Furfural Structures on Pd(111) and Au(111)

The resulting variation of furfural structure as a function of annealing temperature was also investigated. The integrated absorbances of the ~ 1475 and 1465 cm^{-1} modes, which are split because of the presence of different conformers, are plotted versus temperature in Figures 7A for a furfural film on Pd(111) and Fig. 9A on Au(111). They are used to gauge the proportion of each conformer on the surface as a function of annealing temperature. The integrated absorbances of A'' and A' modes are used to measure the average molecular orientation and the combination of these two parameters shows the evolution in furfural's structure, enabling its behavior to be divided into five regions. In region I ($T < 140\text{ K}$), the furfural film structure remains unchanged. In region II ($140\text{ K} < T < 160\text{ K}$), the furfural carbonyl mode absorbance increases, while the intensity of the A'' mode at 784 cm^{-1} decreases, indicating that the furfural C=O group has a vibration with a significant component oriented perpendicularly to the surface. Interestingly, the A' ring mode at 1570 cm^{-1} does not increase in region II, implying that the furyl ring lies relatively parallel to the surface, while the carbonyl group moves away from it, connoting changes in the furfural conformation. In region III, furfural converts from the trans into the cis conformer, in accord with the observation that the cis conformer is the most stable in the solid.¹² The ability to collect data over small temperature intervals allows Arrhenius plots for the temperature dependences of the cis/trans ratios to be obtained for $\sim 47\text{-ML}$ thick films of furfural on Au(111) (Fig. 7D) and on Pd(111) (Fig. 9E) and for a $\sim 9.1\text{-ML}$ film on Pd(111) (Fig. 11C), to yield corresponding energies

of 35.5 ± 2.5 , 32.8 ± 2.5 and 31.5 ± 2.5 kJ/mol. Early infrared and Raman measurements of the enthalpy difference between the furfural conformers estimated a value of ~ 1 kcal/mol (~ 4 kJ/mol),¹² while nuclear magnetic resonance (NMR) measurements yielded ~ 6 kJ/mol, with strong solvent effects.³⁸ A more complete NMR investigation measured reaction enthalpies between 2.6 and 5 kJ/mol, depending on the solvent, with energy barriers between 40 and 49 kJ/mol in solution.³⁹ The energies for cis/trans interconversion on Au(111) are close to the $-CHO$ rotational activation barrier that controls the conformational change for gas-phase furfural of 38.94 kJ/mol.¹³ This indicates that the surface transformation of the conformers is kinetically controlled and that the cis-to-trans interconversion is facilitated by the presence of the surface and may be related to the stabilization of the trans conformer on the surface, resulting in a lower observed energy barrier for the interconversion.⁴⁰ Furfural on Pd(111) has a lower activation barrier than on gold by ~ 2 -3 kJ/mol, which may correlate with the stronger interaction of furfural with palladium than gold.

In region IV (obtained by annealing to 165 K), there is a significant decrease in intensity of all A' modes for thick furfural films on Au(111) and Pd(111), which is accompanied by a substantial increase in intensity of the 783 cm^{-1} A'' modes. This indicates a significant film restructuring to crystallize to form furfural with the plane parallel to the substrate so that vibrational modes with A'' symmetry predominate. The temperature at which furfural crystallizes depends on the initial film thickness and occurs at much lower temperatures in this work than reported previously.⁶ However, as shown in Figure 10, if the film is too thin, the furfural desorbs before crystals can form.

At higher temperatures, in region V (heating to 170 K), the furfural A'' modes decrease in intensity, without observing an increase in modes of A' symmetry, and the TPD results for furfural on Pd(111) (Figure 12) provide insights into the behavior in this region. Furfural desorbs in two

states between 155 and 210 K in a broad, higher-temperature peak centered at ~ 195 K, which saturates in intensity at an exposure of ~ 2.5 L, and a lower-temperature state centered at 173 K, which does not saturate with increasing furfural exposure. The lower-temperature feature is due to multilayer desorption and the higher-temperature peak is assigned to molecular desorption from the furfural monolayer. The furfural multilayer desorption state does not shift with coverage consistent with first-order desorption kinetics. A Redhead analysis,⁴¹ assuming a pre-exponential factor of $1 \times 10^{13} \text{ s}^{-1}$ yields an activation energy for multilayer desorption of ~ 43 kJ/mol, reasonably close to the heat of vaporization of furfural of 44.7 kJ/mol.⁴²

No surface furfural is detected on Au(111) at 170 K, while a furfural monolayer remains on Pd(111) with a similar infrared spectrum to that found after dosing at 90 K, due to the stronger binding of furfural to Pd(111) than to Au(111), but the subsequent behavior of the thin film is identical, independent of the nature of the substrate.

The temperature dependences of the furfural tilt angle are displayed in Figures 7C (Au(111)), 9D (16.7 ML of FF/Pd(111)), and 11B (9.1 ML of FF/Pd(111)), where the furfural tilt angle does not change substantially until ~ 140 K, when it becomes more perpendicular to the surface. This restructuring facilitates the trans-to-cis furfural conversion at 150 K, likely due to the reduction in steric hindrance. Heating to 160 K causes furfural to be more parallel to the surface with an angle of $\sim 10^\circ$, subsequently forming a crystalline structure. Further heating causes furfural to desorb leaving a tilted furfural monolayer on the Pd(111) with a tilt angle of $\sim 40^\circ$, close to the Tilted-2 structure of furfural as predicted by Vlachos.^{31, 32}

XRD has been used to obtain the crystal structure of a thin film of furfural using “in situ cryocrystallography”⁶ and shows that the furfural is present in the cis conformation in the crystal which was formed by annealing to ~ 5 K below the melting temperature (~ 232 K). However, this

temperature is significantly higher than the sublimation temperature of a furfural film (Fig. 12) indicating that the film for which the structure was determined was in equilibrium with the vapor. In this case, the unit cell contains three forms of the furfural molecule and provides more structural detail than infrared spectroscopy. However, the infrared results do indicate that the degree of order in the film depends on its thickness and provides a convenient method for identifying various phases that could be present as a function of film thickness and annealing temperature.

Conclusions

X-ray diffraction of condensed organic layers has been increasingly used to measure the crystal structure of organic films and the work presented here illustrates the use of RAIRS as a rapid method for continuously monitoring the film structure as a function of thickness, annealing temperature and the effect of the nature of the substrate by comparing films on a reactive (Pd(111)) and unreactive (Au(111)) substrate to identify regimes for more detailed structural measurements. This provides an ideal technique for measuring the surface chemistry because it is sensitive to both the local structure through shifts in vibrational frequencies and the orientation because of the surface section rules.⁸ Furthermore, while being surface sensitive, it penetrates sufficiently far into the organic film to investigate the whole film. Furthermore, collecting infrared spectra while simultaneously slowly ramping the sample temperature enables the energetics of various transformations to be measured from temperature-dependent intensity changes.

The furfural monolayer lies flat at low coverages on both Pd(111) and Au(111), but lateral interaction induces the formation of tilted species as the monolayer approaches saturation as a Tilted-2 species predicted by DFT. The furfural geometry changes for multilayer adsorption,

where the average tilt angle of adsorbed furfural increases to finally tends towards a value of 54° due to the formation of a randomly oriented multilayer film at lower temperatures.

Heating the furfural multilayers induces significant structural changes that occur over well-defined temperature ranges. The random film is stable on both substrates up to ~ 140 K, but the furfural tilt increases to $\sim 70^\circ$ as the temperature increases. At the same time, furfural converts from a mixture of cis and trans conformers to a multilayer containing only the cis conformer in a process with an activation energy of ~ 35 kJ/mol. Heating to ~ 160 K causes the furfural to crystallize into a structure in which the planes of the furfural molecules are oriented close to parallel to the substrate on both palladium and gold and the multilayer desorbs at 170 K to removes all furfural from the gold surface, but leaves a saturated furfural monolayer on Pd(111). The temperature-programmed RAIRS experiments provided data that is in accord with the conformational assignments for the crystal structure of furfural previously obtained by cryocrystallography.

Author Contributions

RB and AB collected the experimental data and designed the experiments, NH performed the DFT calculations, RB and QO analyzed the data and made the exposure and temperature-dependent plots, WTT designed the experiments and supervised the project.

Conflicts of Interest

We declare that the authors have no conflicts of interest.

Acknowledgments

We gratefully acknowledge support of this work by the U.S. Department of Energy, Division of Chemical Sciences, Office of Basic Energy Sciences, under grant number DE-FG02-00ER15091.

References

1. P. Mittal, B. Kumar, Y. S. Negi, B. K. Kaushik and R. K. Singh, eds., *Organic Thin Film Transistor Architecture, Parameters and their Applications*, 2011.
2. C. D. Dimitrakopoulos and P. R. L. Malenfant, *Advanced Materials*, 2002, **14**, 99-117.
3. H. Klauk, *Chemical Society Reviews*, 2010, **39**, 2643-2666.
4. A. Salehi, X. Fu, D.-H. Shin and F. So, *Advanced Functional Materials*, 2019, **29**, 1808803.
5. B. Roland, *Zeitschrift für Kristallographie - Crystalline Materials*, 2014, **229**, 595-601.
6. R. W. Seidel, R. Goddard, N. Nöthling and C. W. Lehmann, *CrystEngComm*, 2019, **21**, 3295-3303.
7. O. Panova, C. Ophus, C. J. Takacs, K. C. Bustillo, L. Balhorn, A. Salleo, N. Balsara and A. M. Minor, *Nature Materials*, 2019, **18**, 860-865.
8. R. G. Greenler, *The Journal of Chemical Physics*, 1966, **44**, 310-315.
9. R. G. Greenler, D. R. Snider, D. Witt and R. S. Sorbello, *Surface Science*, 1982, **118**, 415-428.
10. N. B. Colthup, L. H. Daly and S. E. Wiberley, *Introduction to infrared and raman spectroscopy. 2.ed*, Academic Press, New York,N.Y., 1975.
11. M. Rogojerov, G. Keresztury and B. Jordanov, *Spectrochimica Acta Part A: Molecular and Biomolecular Spectroscopy*, 2005, **61**, 1661-1670.

12. G. Allen and H. J. Bernstein, *Canadian Journal of Chemistry*, 1955, **33**, 1055-1061.
13. T. S. Little, J. Qiu and J. R. Durig, *Spectrochimica Acta Part A: Molecular Spectroscopy*, 1989, **45**, 789-794.
14. J. N. Chheda, G. W. Huber and J. A. Dumesic, *Angewandte Chemie-International Edition*, 2007, **46**, 7164-7183.
15. M. J. Climent, A. Corma and S. Iborra, *Green Chemistry*, 2014, **16**, 516-547.
16. I. Delidovich, K. Leonhard and R. Palkovits, *Energy & Environmental Science*, 2014, **7**, 2803-2830.
17. I. Delidovich, P. J. C. Hausoul, L. Deng, R. Pfützenreuter, M. Rose and R. Palkovits, *Chemical Reviews (Washington, DC, United States)*, 2016, **116**, 1540-1599.
18. J. W. Medlin, *ACS Catalysis*, 2011, **1**, 1284-1297.
19. J. C. Serrano-Ruiz and J. A. Dumesic, *Energy & Environmental Science*, 2011, **4**, 83-99.
20. J.-P. Lange, E. van der Heide, J. van Buijtenen and R. Price, *ChemSusChem*, 2012, **5**, 150-166.
21. A. Bohre, S. Dutta, B. Saha and M. M. Abu-Omar, *ACS Sustainable Chemistry & Engineering*, 2015, **3**, 1263-1277.
22. R. Mariscal, P. Maireles-Torres, M. Ojeda, I. Sadaba and M. Lopez Granados, *Energy & Environmental Science*, 2016, **9**, 1144-1189.
23. M. Kaltchev, A. W. Thompson and W. T. Tysoe, *Surface Science*, 1997, **391**, 145-149.
24. G. Kresse and J. Furthmüller, *Physical Review B*, 1996, **54**, 11169-11186.
25. G. Kresse and J. Furthmüller, *Computational Materials Science*, 1996, **6**, 15-50.
26. J. P. Perdew, K. Burke and M. Ernzerhof, *Physical Review Letters*, 1996, **77**, 3865.

27. S. Grimme, J. Antony, S. Ehrlich and H. Krieg, *The Journal of Chemical Physics*, 2010, **132**, 154104.
28. H. J. Monkhorst and J. D. Pack, *Physical Review B*, 1976, **13**, 5188-5192.
29. K. Momma and F. Izumi, *Journal of Applied Crystallography*, 2011, **44**, 1272-1276.
30. G. Schultz, I. Fellegvári, M. Kolonits, Á. I. Kiss, Bélapete and J. Bánki, *Journal of Molecular Structure*, 1978, **50**, 325-343.
31. V. Vorotnikov, G. Mpourmpakis and D. G. Vlachos, *Acs Catalysis*, 2012, **2**, 2496-2504.
32. S. Wang, V. Vorotnikov and D. G. Vlachos, *ACS Catalysis*, 2015, **5**, 104-112.
33. J. L. Davis and M. A. Barteau, *J. Am. Chem. Soc.*, 1989, **111**, 1782-1792.
34. J. L. Davis and M. A. Barteau, *Surface Science*, 1990, **235**, 235-248.
35. C. D. Craver and S. Coblentz, *The Coblentz Society desk book of infrared spectra*, The Society, Kirkwood, MO (P.O. Box 9952, Kirkwood 63122), 1982.
36. H. Hoffmann, F. Zaera, R. Mark Ormerod, R. M. Lambert, W. Lu Ping and W. T. Tysoe, *Surface Science*, 1990, **232**, 259-265.
37. W. T. Tysoe, R. M. Ormerod, R. M. Lambert, G. Zgrablich and A. Ramirez-Cuesta, *The Journal of Physical Chemistry*, 1993, **97**, 3365-3370.
38. R. J. Abraham and T. M. Siverns, *Tetrahedron*, 1972, **28**, 3015-3024.
39. A. D. Bain and P. Hazendonk, *The Journal of Physical Chemistry A*, 1997, **101**, 7182-7188.
40. M. G. Evans and M. Polanyi, *Transactions of the Faraday Society*, 1938, **34**, 11-24.
41. P. A. Redhead, *Vacuum*, 1962, **12**, 203-211.
42. R. M. Stephenson and S. Malanowski, *Handbook of the thermodynamics of organic compounds*, Elsevier, New York, 1987.

Figure Captions

Figure 1: Depictions of the O-O cis and O-O trans structures of furfural

Figure 2: Reflection-absorption infrared (RAIRS) spectra of furfural adsorption on clean Au(111) held at 130 K as a function of exposure in Langmuir (L), where the exposures are indicated adjacent to the corresponding spectrum.

Figure 3: Plots of (a) integrated absorbances of selected A' and A'' modes versus exposure, (b) the percent of cis and trans furfural present as a function of exposure, (c) the vibrational frequency for the carbonyl vibration mode for cis and trans furfural versus exposure, (d) the average tilt angle calculated for furfural versus exposure onto clean Au(111) at 130 K.

Figure 4: Reflection-absorption infrared (RAIRS) spectra of furfural adsorption on clean Pd(111) held at 90 K as a function of exposure in Langmuir (L), where the exposures are indicated adjacent to the corresponding spectrum.

Figure 5: Plots of (a) integrated absorbance of selected A' and A'' modes versus exposure, (b) integrated absorbance of selected A' and A'' modes versus exposure over a larger range, (c) the percent of cis and trans furfural present as a function of exposure, and (d) the average tilt angle calculated for furfural versus exposure onto clean Pd(111) at 90 K.

Figure 6: Reflection-absorption infrared (RAIRS) spectra of 140.9 L of furfural adsorbed on a clean Au(111) at 130 K as a function of annealing temperature, where the temperatures are indicated adjacent to the corresponding spectrum.

Figure 7: Plots of (a) integrated absorbances of the cis and trans splitting of vibrational modes at 1470 cm^{-1} versus temperature, (b) the relative proportion of the cis and trans conformers of furfural versus temperature, (c) the average tilt angle of furfural as a function of temperature and (d) a plot of the $\ln\left(\frac{I(cis)}{I(trans)}\right)$ versus $\frac{1}{T}$ for furfural adsorbed on a clean Au(111) at 130 K heated to various temperatures.

Figure 8: Reflection-absorption infrared (RAIRS) spectra of 47 L of furfural adsorbed on a clean Pd(111) at 90 K as a function of annealing temperature, where the temperatures are indicated adjacent to the corresponding spectrum.

Figure 9: Plots of (a) the integrated absorbances of the cis/trans splitting of vibrational modes at 1470 cm^{-1} versus temperature (b) the relative proportion of the cis and trans conformers of furfural versus temperature, (c) the cis:trans ratio of furfural versus temperature over a larger range, (d) the average furfural tilt angle relative to the surface vs temperature, and (e) plot of the $\ln\left(\frac{I(cis)}{I(trans)}\right)$ versus $\frac{1}{T}$ for furfural adsorbed on a clean Pd(111) at 90 K heated to various temperatures.

Figure 10: Reflection-absorption infrared (RAIRS) spectra of 27.2 L of furfural adsorbed on a clean Pd(111) at 90 K as a function of annealing temperature, where the temperatures are indicated adjacent to the corresponding spectrum.

Figure 11: Plots of (a) the relative proportion of cis and trans species of furfural as a function of temperature, (b) the average tilt angle relative to the surface as a function of temperature, and (c)

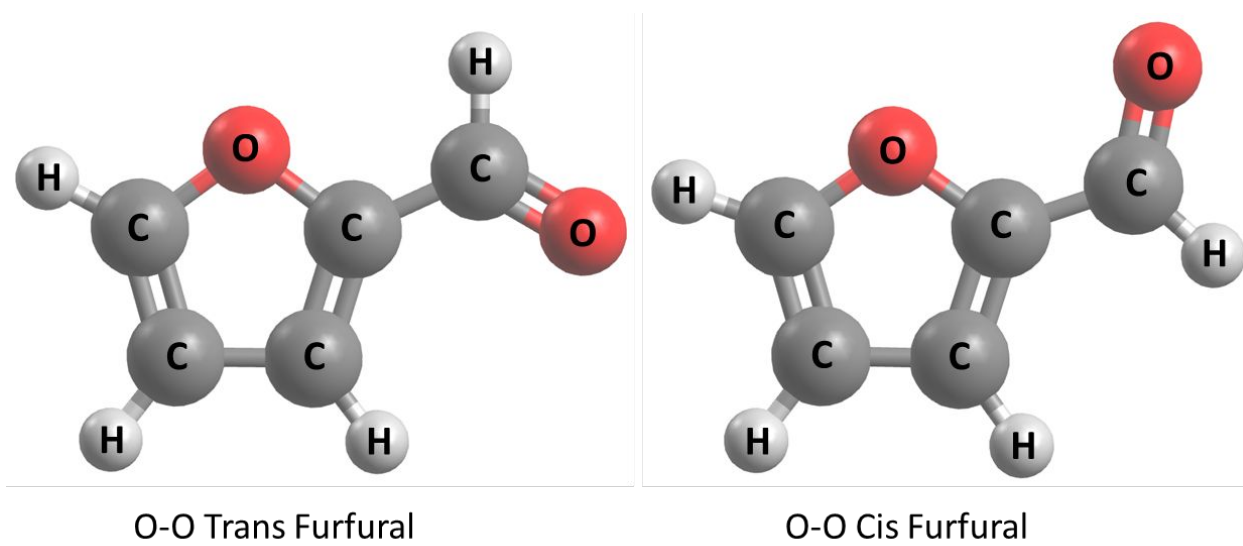
plot of the $\ln \left(\frac{I(cis)}{I(trans)} \right)$ versus $\frac{1}{T}$ for furfural adsorbed on a clean Pd(111) at 90 K as a function of temperature.

Figure 12: Temperature-programmed desorption of furfural from Pd(111) obtained by monitoring the 96 amu signal using a heated rate of 5 K/s as a function of exposure, where the exposures in Langmuirs are indicated adjacent to the corresponding spectrum.

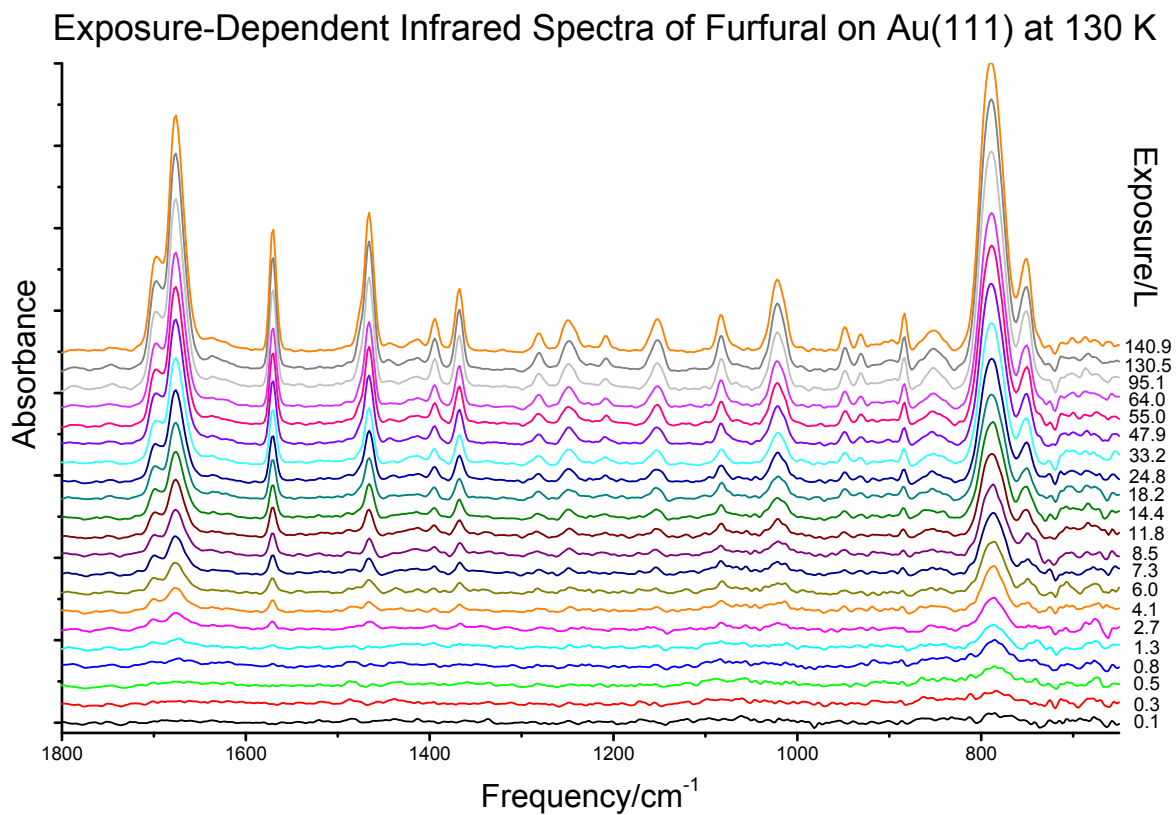
Tables

Mode Number	DFT Calculations Frequency/cm ⁻¹		Gas-phase Furfural Frequency/cm ⁻¹		Furfural Multilayer on Pd(111)/cm ⁻¹		Symmetry	I/P or O/P	Assignment
	Trans	Cis	Trans	Cis	Trans	Cis			
1 f	3217	3214	3134	3124	3137	3137	A'	In	C-H ring stretch
2 f	3203	3195						In	C-H ring stretch
3 f	3189	3186						In	C-H ring stretch
4 f	2841	2821	2855	2813	2856	2856	A'	In	Aldehyde C-H C-H stretch
5 f	1690	1697	1675	1692	1677	1703	A'	In	C=O stretch
6 f	1559	1550	1569	1565	1571	1571	A'	In	Ring mode
7 f	1456	1464	1465	1474	1465	1475	A'	In	Ring mode
8 f	1400	1393	1394	1394	1394	1394	A'	In	Ring mode
9 f	1358	1347	1367	1367	1367	1367	A'	In	Aldehyde C-H Rocking
10 f	1239	1209	1246	1222	1251	1230	A'	In	C-H Rocking
11 f	1184	1271	1208	1278	1207	1279	A'	In	Ring mode
12 f	1156	1164	1149	1157	1153	1153	A'	In	Ring mode
13 f	1096	1089	1083	1077	1085	1084	A'	In	Ring C-H Rock
14 f	1016	1023	1015	1021	1021	1021	A'	In	Ring C-H Scissor
15 f	973	964						Out	Aldehyde C-H Wag
16 f	933	919	946	930	947	929	A'	In	Ring mode
17 f	893	883						Out	Ring C- H Twist
18 f	877	876	883	883	884	884	A'	In	Ring mode
19 f	830	823	842	842	842	842	A''	Out	Ring C-H Twist
20 f	755	755	768	768	789	789	A''	Out	Ring C-H Wag
21 f	736	744	747	755	755	755	A'	In	-
22 f	630	642						Out	Ring
23 f	602	598						Out	Ring

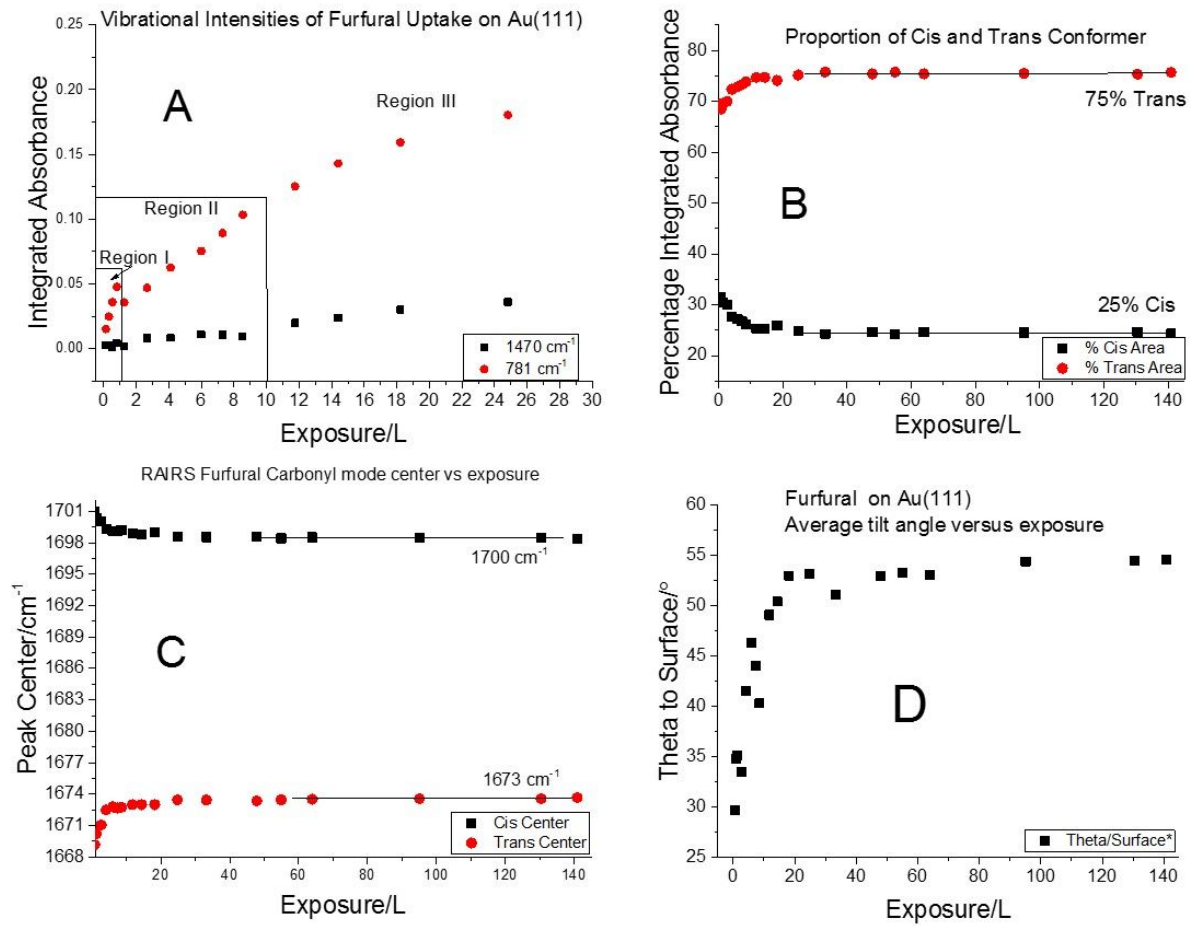
Table 1: The infrared vibrational model for molecular furfural that compares the results of density functional theory calculations with the vibrational frequencies found for gas-phase furfural^{11, 12, 30} and with furfural multilayers after a 46.8 L exposure on Pd(111). Also shown are the irreducible representation of the normal modes within the C_s point group, and whether the normal modes lie within or perpendicular the molecular plane are indicated. Finally, the mode descriptions are indicated.



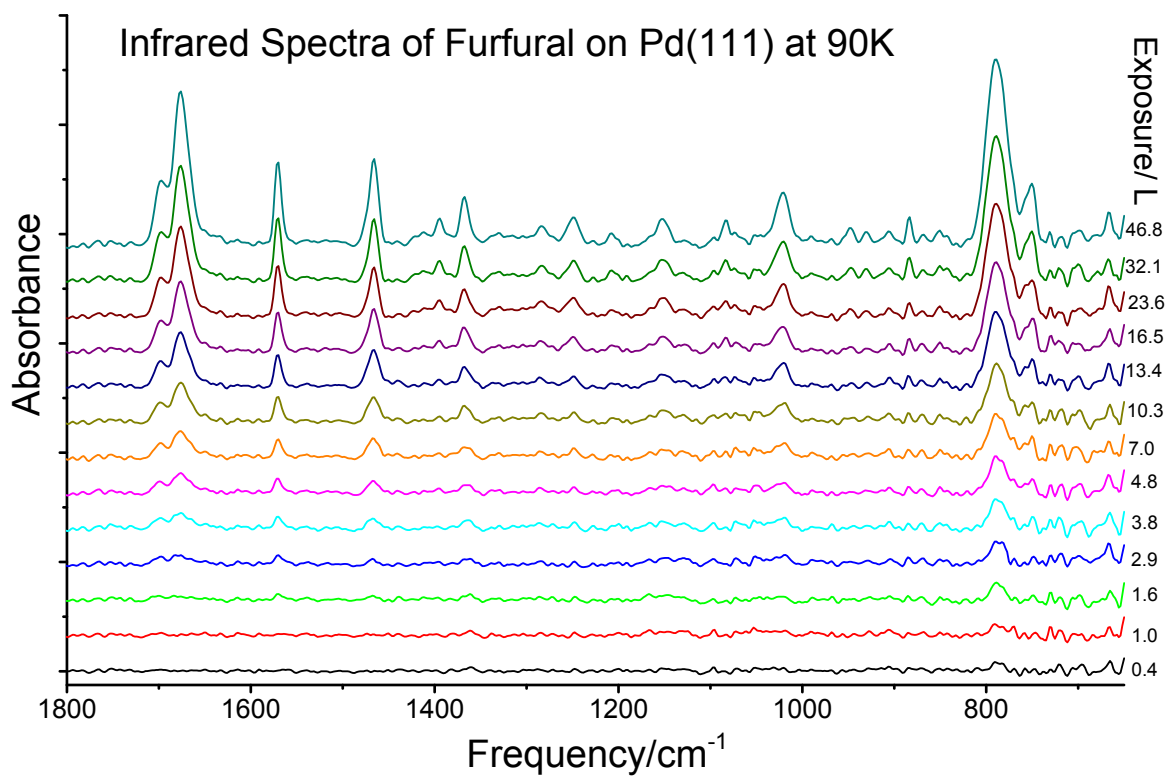
Bavisotto et al, Figure 1



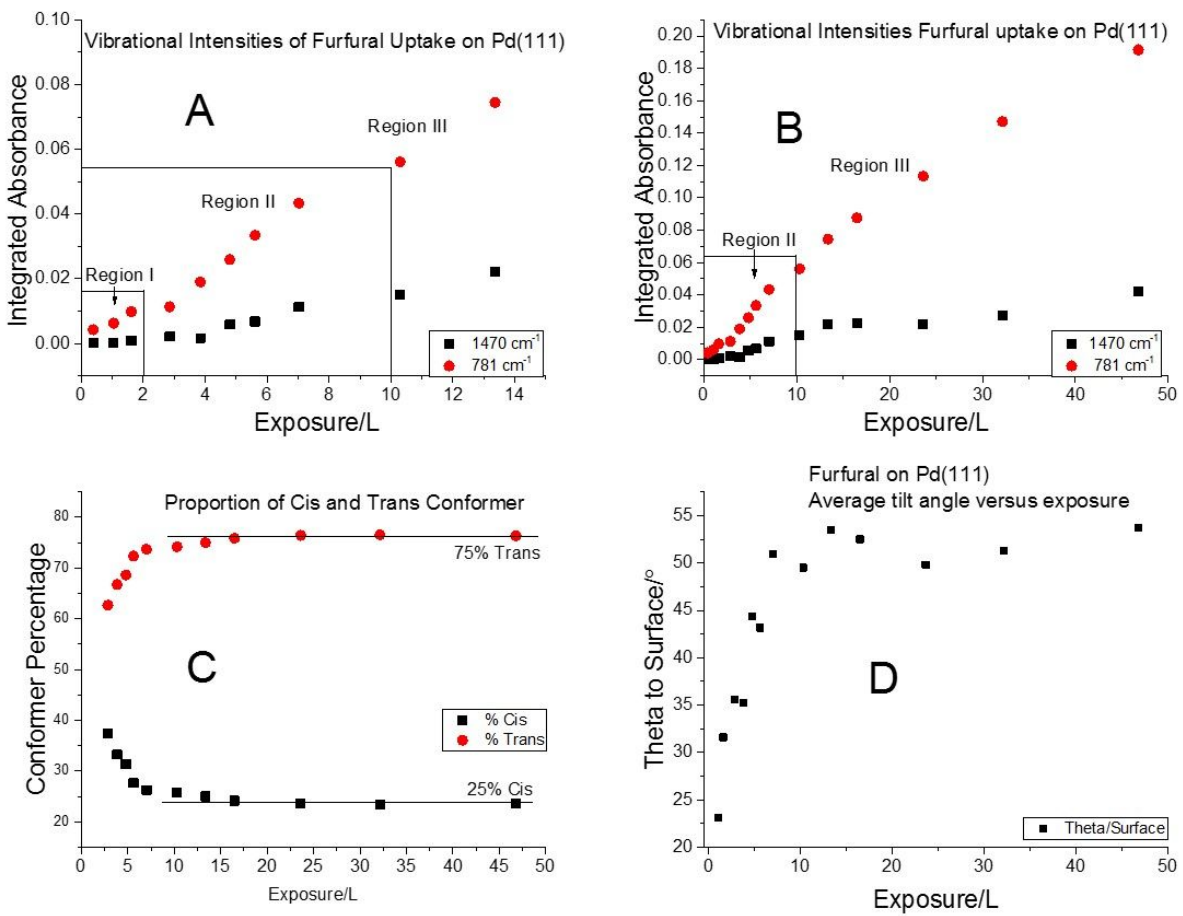
Bavisotto et al, Figure 2



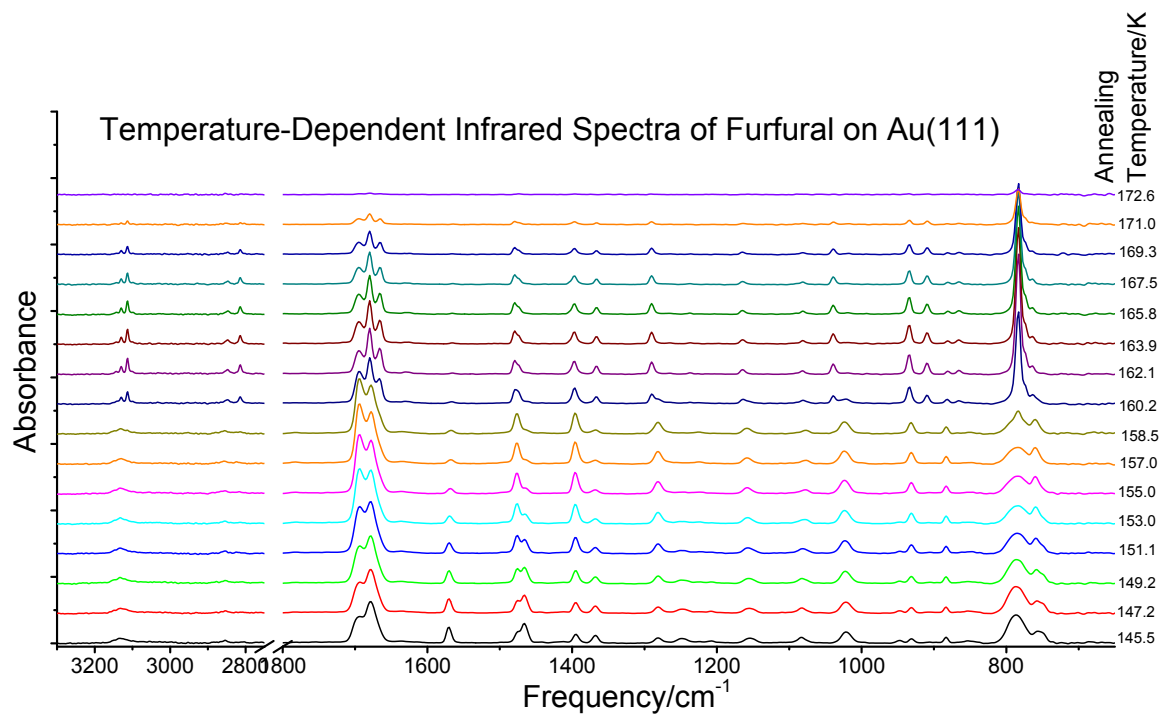
Bavisotto et al, Figure 3



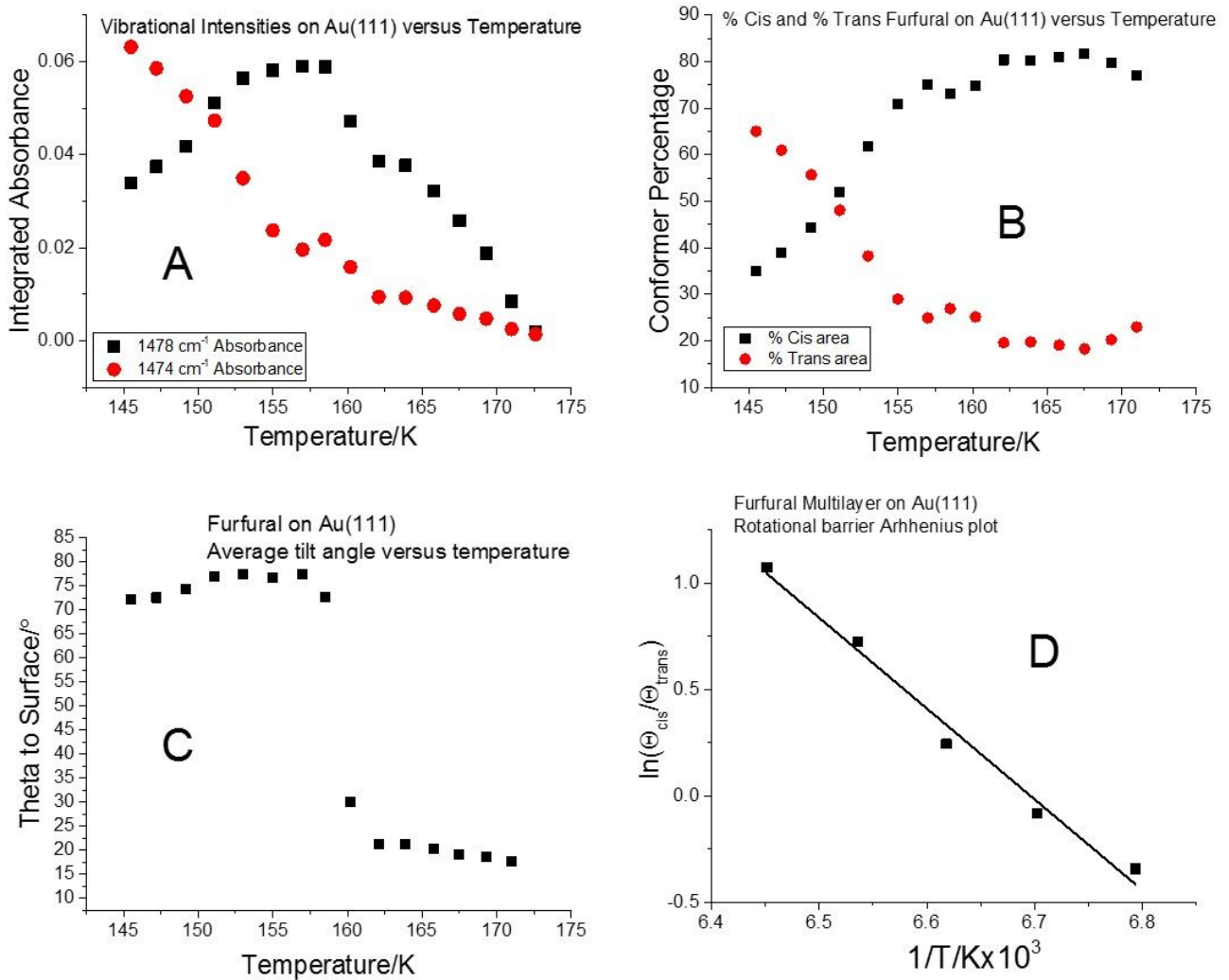
Bavisotto et al, Figure 4



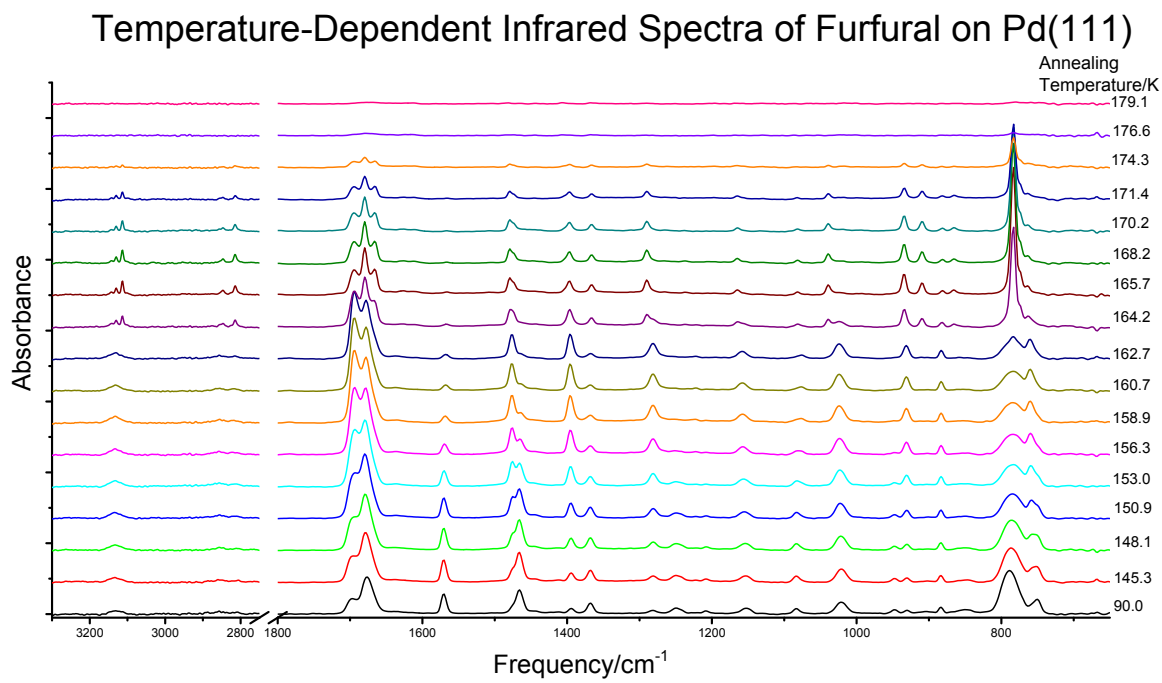
Bavisotto et al, Figure 5



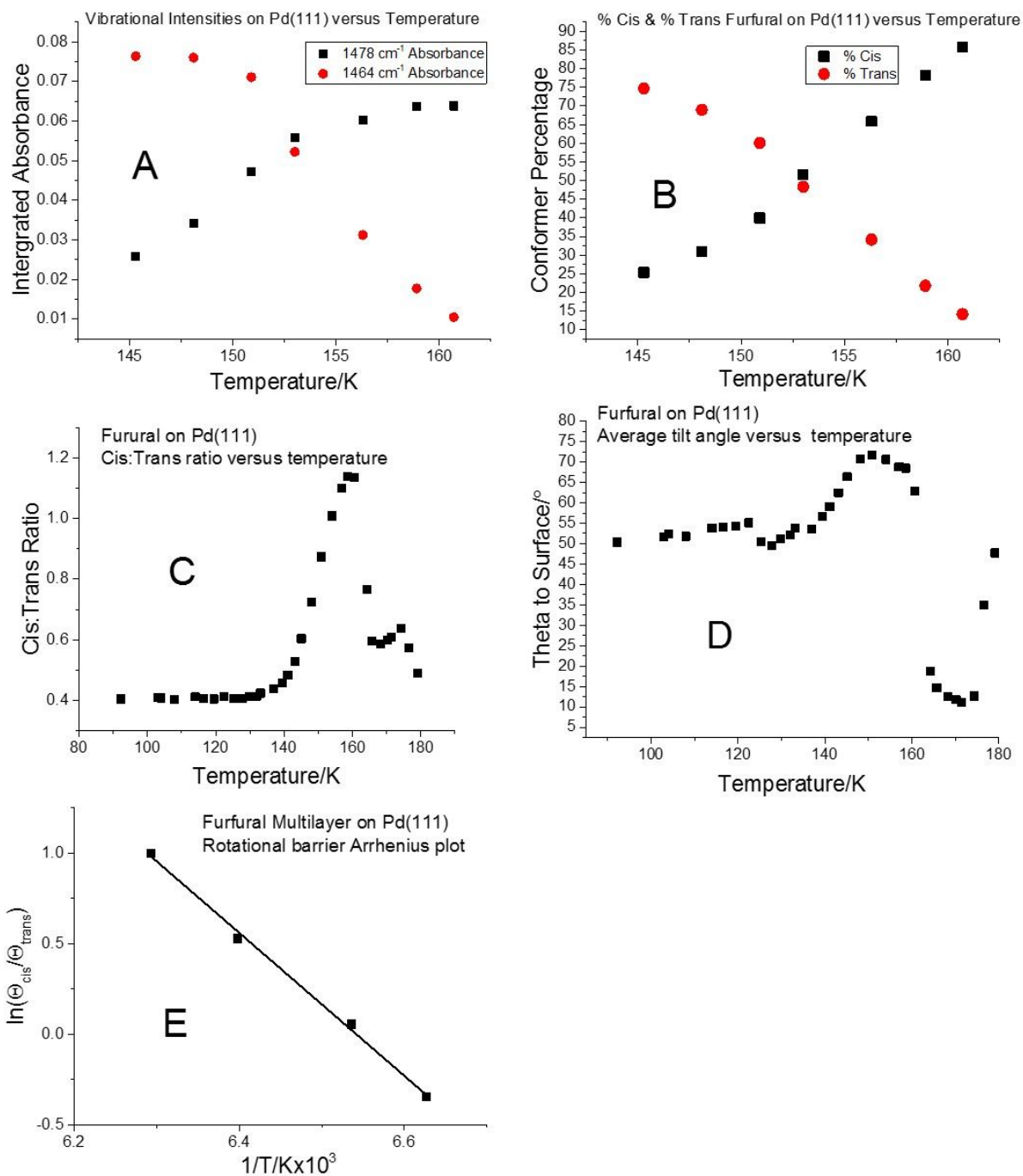
Bavisotto et al, Figure 6



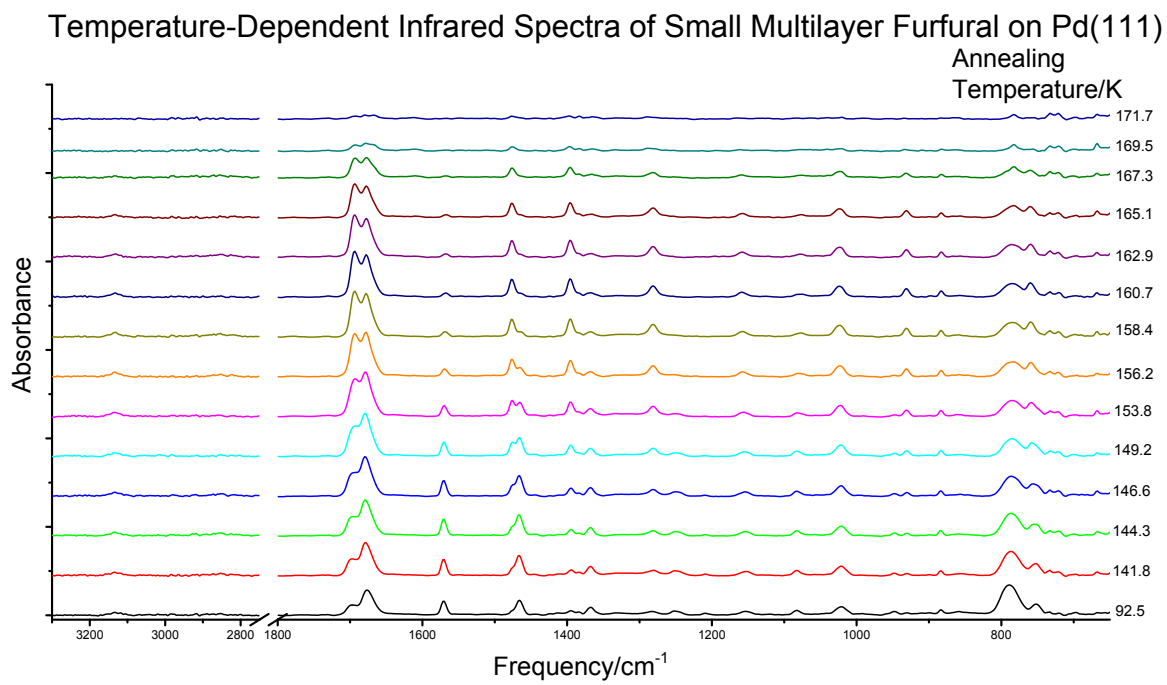
Bavisotto et al, Figure 7



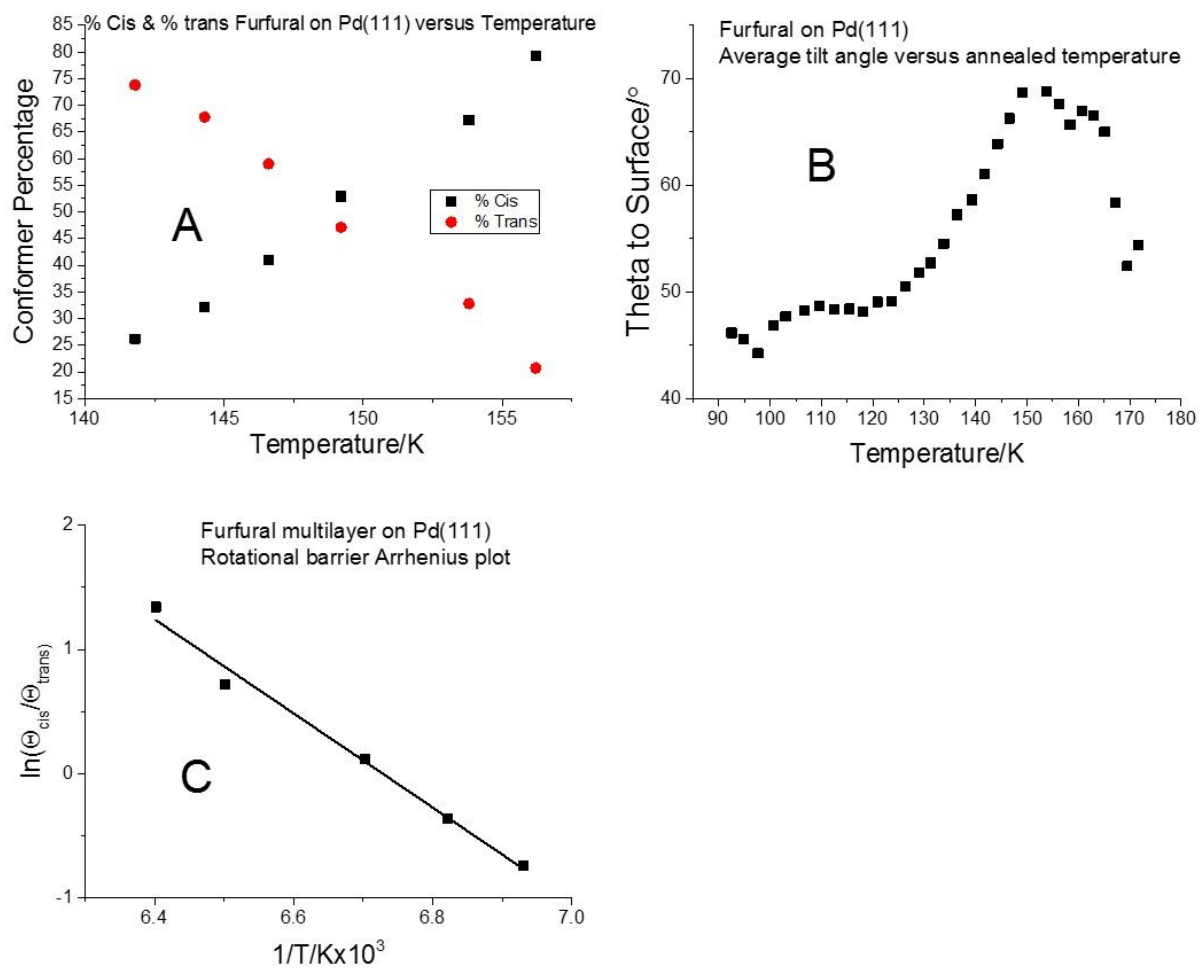
Bavisotto et al, Figure 8



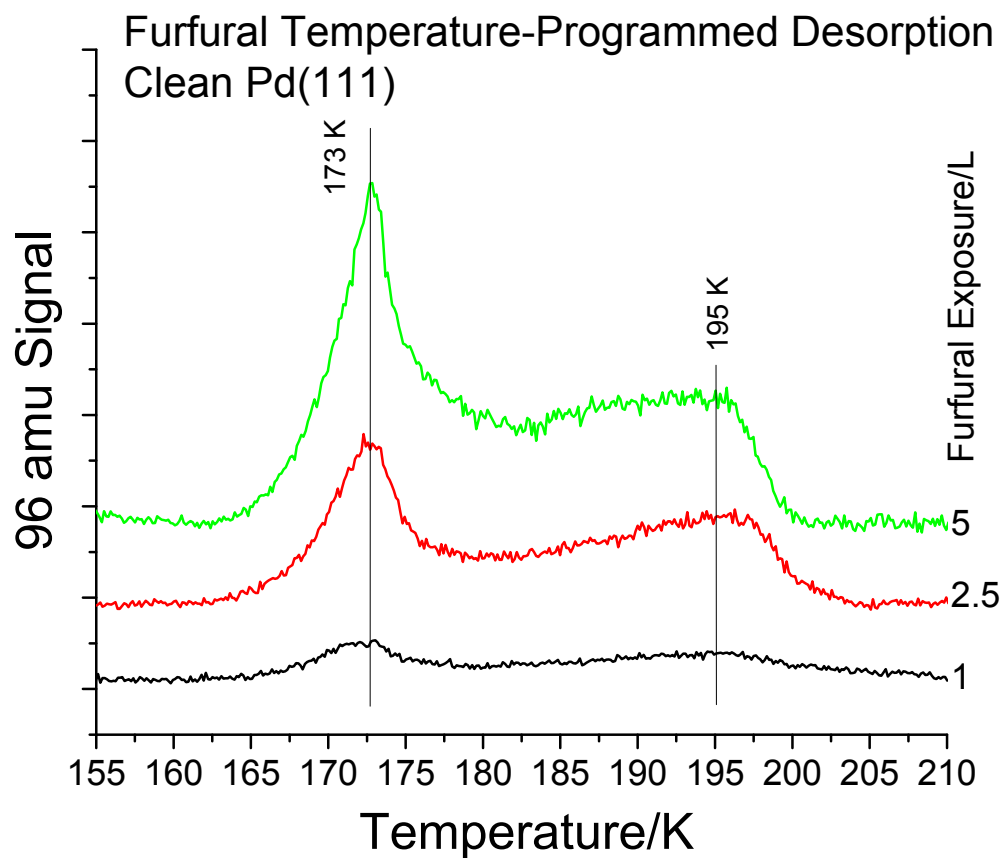
Bavisotto et al, Figure 9



Bavisotto et al, Figure 10



Bavisotto et al, Figure 11



Bavisotto et al, Figure 12